Comparison of Quinone-Based Catholytes for Aqueous Redox Flow Batteries and Demonstration of Long-Term Stability with Tetrasubstituted Quinones

*James B. Gerken, Colin W. Anson, Yuliya Preger, Peter G. Symons, J. David Genders, Yang Qiu, Wenzhen Li, Thatcher W. Root, and Shannon S. Stahl**

Quinones are appealing targets as organic charge carriers for aqueous redox flow batteries (RFBs), but their utility continues to be constrained by limited stability under operating conditions. The present study evaluates the stability of a series of water-soluble quinones, with redox potentials ranging from 605–885 mV versus NHE, under acidic aqueous conditions (1 M H_2SO_4). Four of the quinones are examined as cathodic electrolytes in an aqueous RFB, paired with anthraquinone-2,7-disulfonate as the anodic electrolyte. The RFB data complement other solution stability tests and show that the most stable electrolyte is a tetrasubstituted quinone containing four sulfonated thioether substituents. The results highlight the importance of substituting all C–H positions of the quinone in order to maximize the quinone stability and set the stage for design of improved organic electrolytes for aqueous RFBs.

1. Introduction

Redox flow batteries (RFBs) are attracting considerable interest due to their potential utility for grid-scale energy storage.[1,2] This type of battery typically features an electrolysis cell fed from two tanks containing soluble redox-active species, one low-potential and one high-potential. Both oxidation states of both species must exhibit, among other properties, high stability and high solubility in a medium of high ionic conductivity.[3,4] An aqueous acidic medium offers many advantages (low cost, high

ionic conductivity, good membrane performance) and has been used in the largest-scale flow batteries installed to date[1,4] using inorganic electrolytes, such as vanadium salts.[5] Compared to inorganic compounds, organic electrolytes hold the promise of near-limitless availability and (bio)degradability into benign products.[6,7] One class of redox-active organic compounds that has attracted much research is quinones, which undergo $2e^-/2H^+$ reduction over a wide range of potentials based on their ancillary substitution.[8–11] It is thus possible to select two quinones with different reduction potentials as the low- and high-potential mediators in a RFB (**Scheme 1**).[12]

Anthraquinone derivatives, such as anthraquinone-2,7-disulfonate (AQDS), have proven to be quite effective as low-potential (anodic) electrolytes, and they have been paired with both organic and inorganic high-potential (cathodic) electrolytes in aqueous RFBs.[10,13–19] The lower stability of high potential quinones has limited the utility of quinone-based catholytes, as revealed by studies with the parent benzoquinone,[20] as well as benzoquinones bearing substitutents that increase their aqueous solubility[14–18] (inter alia, compounds **1–3** in **Scheme 2**). Benzoquinones are reactive electrophiles, and they are capable of undergoing Michael addition with various nucleophiles, including water, as well as oligomerization.[14,15,21] Recognition of this issue provided the basis for Narayanan and co-workers to develop the trisubstituted quinone **3**, which exhibits considerably improved stability relative to previously reported derivatives **1** and **2** (Scheme 2).[14]

We recently reported the design of tetra-substituted quinones containing four sulfonated thioether substituents, compounds **4** and **5**, which display substantially enhanced stability relative to quinones **1–3** in preliminary chemical stability tests.[22,23] Herein, we report related quinones (compounds **6** and **7**) and conduct stability tests of the entire series of quinones in Scheme 2 to elucidate the factors that contribute to improved mediator stability. These solution-phase tests are complemented by flow battery testing of quinones **1–4**. Collectively, the results show that tetrasubstitution of the quinone, as in **4**, greatly enhances quinone stability and that the thioether linkage is resistant to substitution over prolonged periods in aqueous acid at elevated temperature. An all-organic RFB with

Dr. J. B. Gerken, Dr. C. W. Anson, Prof. S. S. Stahl
Department of Chemistry
University of Wisconsin–Madison
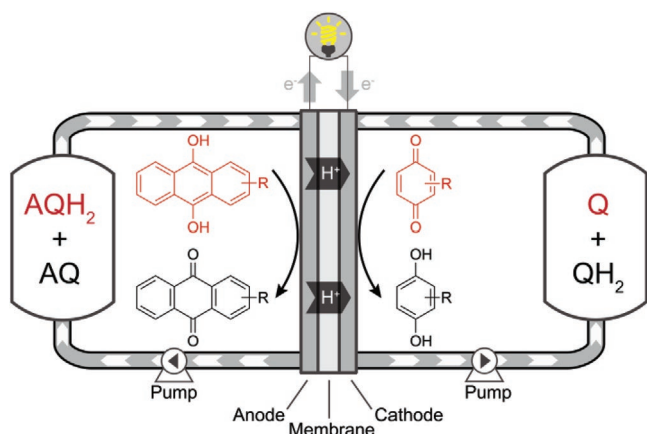1101 University Avenue, Madison, WI 53706-1322, USA
E-mail: stahl@chem.wisc.edu
Dr. Y. Preger, Prof. T. W. Root
Department of Chemical and Biological Engineering
University of Wisconsin–Madison
1415 Engineering Drive, Madison, WI 53706, USA
Dr. P. G. Symons, Dr. J. D. Genders
Electrosynthesis Company, Inc
72 Ward Road, Lancaster, NY 14086, USA
Dr. Y. Qiu, Prof. W. Li
Department of Chemical and Biological Engineering
Iowa State University
2114 Sweeney Hall, 618 Bissell Road, Ames, IA 50011-2230, USA

The ORCID identification number(s) for the author(s) of this article can be found under https://doi.org/10.1002/aenm.202000340.

ADVANCED
SCIENCE NEWS
www.advancedsciencenews.com

ADVANCED
ENERGY
MATERIALS
www.advenergymat.de

Scheme 1. All-quinone redox flow battery (in discharge mode). AQH_2, AQ = reduced and oxidized forms of an anthraquinone with a low reduction potential; QH_2, Q = reduced and oxidized forms of a high-potential quinone.

quinone **4** as the catholyte and AQDS as the anolyte demonstrates current densities of 800 mA cm^{-2} and a power density of >100 mW cm^{-2} (180 mW cm^{-2} iR-corrected). The insights from this study showcase structural properties of high-potential quinones that could lead to more effective performance and potential practical utility.

2. Results and Discussion

2.1. Synthesis of Thioether Hydroquinones

Hydroquinones **1** and **2** are commercially available as the sodium and potassium salts, respectively, and compounds **3**, **4**, **5**, and **8** were synthesized according to literature procedures (in some cases, with modifications; see Supporting Information).[14,23,24] Hydroquinones **6** and **7** were synthesized by addition of sodium mercaptoethanesulfonate to benzoquinone. The tris-thioether compound **6** is an analogue of the major byproduct formed during the previously reported synthesis of **4**,[22] and it was produced by attempting the synthesis of **5** at elevated temperature (see Supporting Information). The yield of the byproduct was instead improved, allowing **6** to be isolated for further studies. The mono-thioether compound **7** was synthesized by simultaneous addition of benzoquinone and the thiol to the reaction so as to minimize the amount of reoxidation of the monosubstituted adduct (see Supporting Information).

2.2. CV Analysis and Quinone Stability Testing in Solution

Cyclic voltammograms (CVs) of the quinones depicted in Scheme 2 are shown in **Figure 1** (see also, **Table 1** and Figure S12, Supporting Information). As expected, direct attachment of an electron-withdrawing sulfonate group to the quinone ring raises the potential, although this effect is offset in compound **3** by the two methyl groups that are also present. The potential difference between disulfonated compounds **1** and **8** is typical
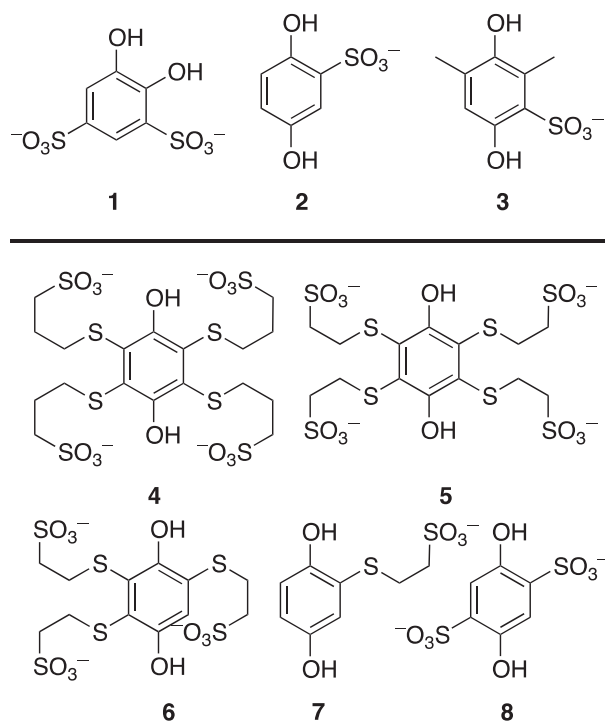
Scheme 2. Compounds investigated in this study as potential RFB cathode mediators.

for similarly-substituted *ortho*- and *para*-benzoquinones. The CV data also show that thioether substituents are mildly electron-donating, leading to a small decrease in potential on further substitution from **7** through **6** to **5**.

The hydroquinones **1–8** were oxidized chemically to the corresponding quinones using a modification of Kochi's previously
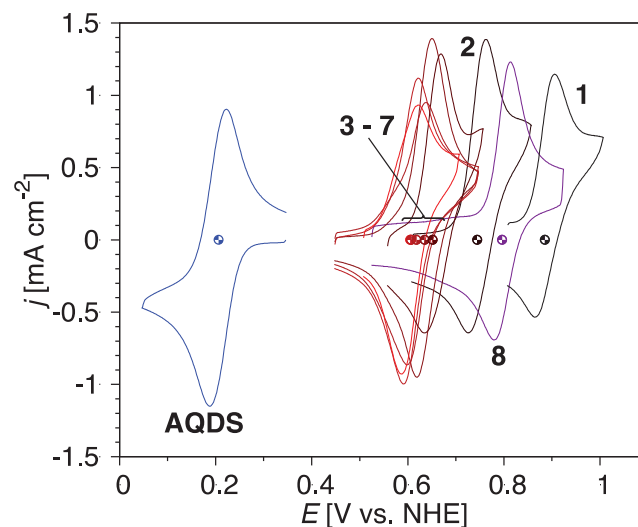

Figure 1. Cyclic voltammograms of compounds **1–8**, and AQDS. Reduction potentials of each compound are indicated by dots in the graph. Voltammograms were acquired at 5 mM concentration in 1 M H_2SO_4 at 10 mV s^{-1} at an MWCNT-coated glassy carbon electrode (see Supporting Information for details).[25]

Table 1. Quinone reduction potentials and half-lives.

Compound	$E_{1/2}$ [V vs NHE][a]	$t_{1/2}$ [h][b]
1	0.885	<0.05
2	0.744	1.5
3	0.652	37.5
4	0.605	5120
5	0.618	3860
6	0.607	322
7	0.635	6.1
8	0.796	n.d.[c]

[a] In 1 M H_2SO_4; [b] In 0.5 M D_2SO_4, 60 °C; [c] Not determined.

reported NO_x-based method (see Supporting Information for details).[22,26] With the isolated quinones in hand, we examined the stability of the quinone forms of **5**, **6**, and **7** using a ^1H NMR spectroscopic protocol, similar to that previously used with compounds **1–4**.[22] Briefly, samples of each quinone were prepared in 0.5 M D_2SO_4 with 0.05 M CH_3SO_3H as an internal standard, and the fate of each quinone was monitored by ^1H NMR spectroscopy. A half-life for the [quinone] + [hydroquinone] mass balance was obtained for each compound (**Figure 2**a and Table 1; Figures S9–S11, Supporting Information). No trace is shown for compound **1** since its quinone had fully decomposed by the first time point (15 min), and the oxidation product of **8** was observed to be unstable at room temperature and was not investigated further (for characterization of the reaction product, see Supporting Information). The mass balance for compounds **2** and **3** do not decay to zero because some of their decomposition products are able to reduce the remaining quinone to the hydroquinone, which is stable under the test conditions (cf. Scheme S2, Supporting Information).[22]

The NMR data show that greater substitution is associated with greater stability, with a profound increase on going from tri- to tetrasubstituted (note the log scale time axis in Figure 2a). As noted above, the effect on quinone reduction potential of increasing number of thioether substituents is modest. The similar reduction potentials of compounds **3–7** are useful for assessing the effect of substitution on kinetic stability in the absence of large thermodynamic differences. Combining the new and previously-reported[22] solution half-life data on **1–7** with reduction potentials obtained by cyclic voltammetry (vide supra) reveals a marked advantage for tetrasubstitution by thioethers, even over less-substituted quinones with similar reduction potentials and substituent types (Figure 2b and Table 1).

2.3. Flow Battery Comparison

For a flow battery, high cathode reduction potentials and low anode reduction potentials are desirable, explaining the previous interest in compound **1**.[10,17] Due to its adequate solubility, commercial availability in pure form, and acceptable reduction potential, we selected anthraquinone-2,7-disulfonate (AQDS) as the anode compound for flow battery studies.[27] Compound **4** was selected for the cathode over compound **5** due to the lower

cost of its precursor.[28] To compare the properties of different quinones in a full flow battery, a system was constructed with peristaltic pumps circulating anode and cathode fluids between separate flasks and a 5 cm^2 membrane/electrode assembly held at 60 °C (Figure S17, Supporting Information). The cathode solution consisted of 4 mmol of the hydroquinone in question dissolved in 20 mL of 1 M H_2SO_4 (0.2 M quinone). The anode solution consisted of 13 mmol of anthraquinone-2,7-disulfonate and 2 mmol of anthrahydroquinone-2,7-disulfonate dissolved in 75 mL of 1 M H_2SO_4 (see Supporting Information and below for details and discussion). This buffered excess of anode solution minimizes the effect of any changes thereto, such as anthrahydroquinone decomposition,[29] on the system as a whole. By selecting a concentration of 0.2 M of each redox-active species in 1 M H_2SO_4, it was possible to use the salt form of each compound without ion-exchanging it prior to the experiment. This uniform set of conditions was designed to benchmark the stability of different mediators during charge–discharge cycling.
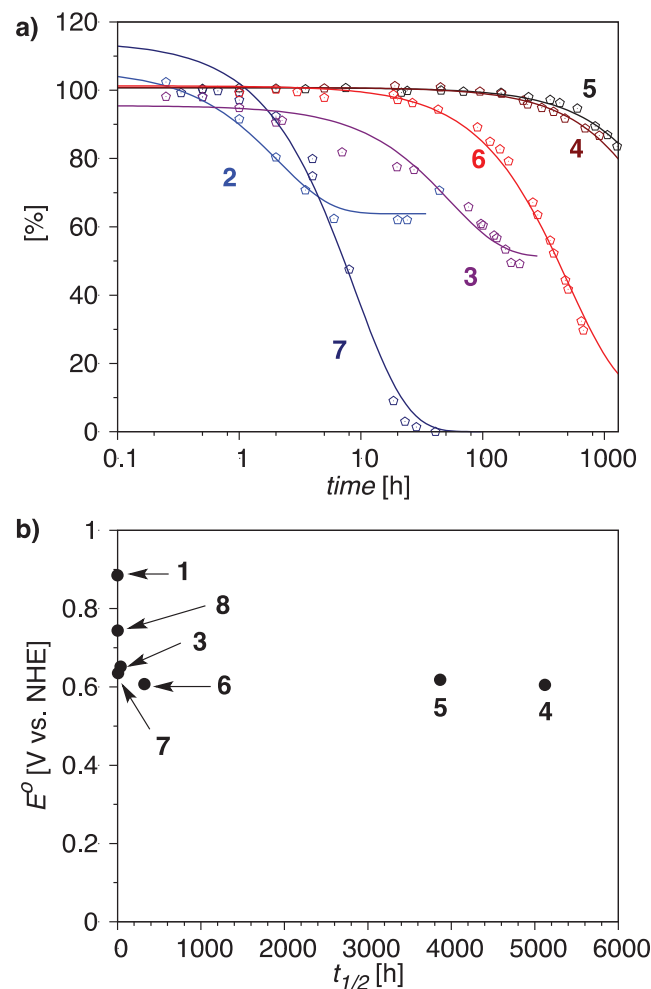

Figure 2. a) Time course experiments tracking the fate of the quinones **2–7** in 0.5 M D_2SO_4 in D_2O with 0.05 M CH_3SO_3H as an internal standard at 60 °C. For discussion of the fitted lines, see Supporting Information. b) Half-lives of quinones versus $E°$ for quinones **1–8**. Redox potentials were measured in 1 M H_2SO_4 at room temperature, while half lives were measured by ^1H NMR spectroscopy in 0.5 M D_2SO_4 in D_2O with 0.05 M CH_3SO_3H as an internal standard at 60 °C. A $t_{1/2}$ of <3 min was estimated for quinone **1**.

**ADVANCED
SCIENCE NEWS**
www.advancedsciencenews.com

**ADVANCED
ENERGY
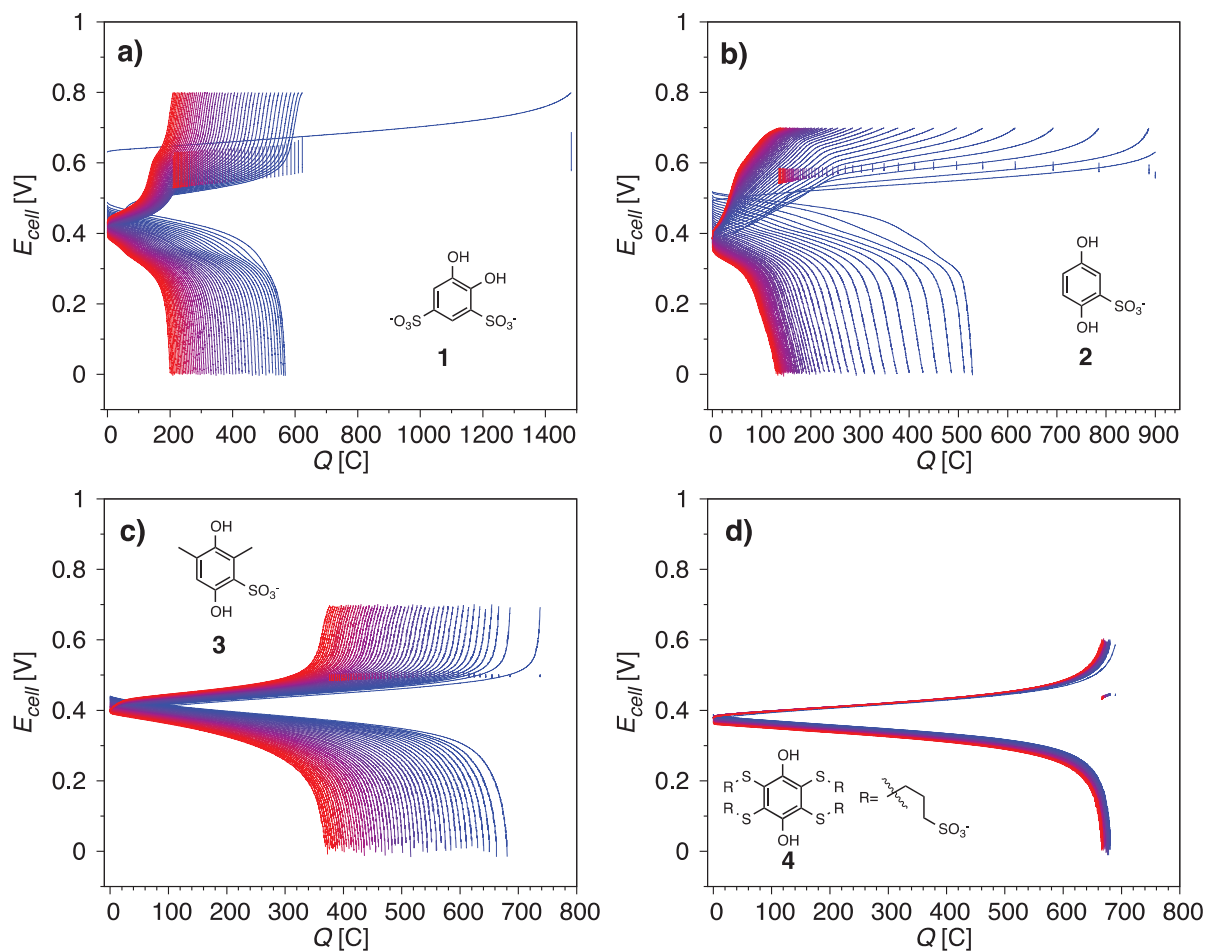MATERIALS**
www.advenergymat.de

Figure 3. Charge–discharge curves for flow batteries constructed with different cathode species and AQDS at the anode. The theoretical capacity in each case is 771.9 C. Each cell was cycled for 50 charge-hold-discharge cycles, with vertical lines indicating the change in open-circuit potential during the hold period (blue = cycle 1, red = cycle 50).

The cycling protocol began with charging the cell at 50 mA cm^{-2} until a cutoff potential was reached at 200 mV above the expected cell potential (based on CV data). Thus prepared, the flow battery was held at open circuit before being discharged.[30] This hold period serves two purposes. First, it reflects the fact that many use cases for RFBs require their ability to hold charge. Second, the increased time spent in the charged state amplifies the differences in chemical stability between quinones, allowing for those differences to become apparent over fewer charge–discharge cycles. Similarly, performing the tests at elevated temperatures accelerated the aging of the electrolytes.

Finally, the cell was discharged to 0 V at 50 mA cm^{-2} and the charge-hold-discharge process was repeated for 50 charge–discharge cycles. From the plots of the charge–discharge curves, differences between compounds **1–4** are readily apparent (**Figure 3**). Compound **1** releases 3.8 e$^-$ mol^{-1} on its initial charge. The origin of this stoichiometry is discussed further below, but the initial charging takes place at a cell potential commensurate with the difference in reduction potential between **1** and AQDS derived from CV measurements. In contrast, the discharge takes place at a significantly lower potential

and consumes less than 2 e$^-$ mol^{-1}. Charging in subsequent cycles takes place at a potential much lower than expected for a **1**/AQDS redox couple, with the appearance of a second potential plateau at even lower potential later in the cycling test. Compound **2** shows similar overcharging, albeit to a lesser degree than compound **1**. Subsequent charging cycles with **2** show the appearance of current at lower potentials, similar to that observed for **1** and presumably for similar reasons (see further discussion below). However, in neither case is a discharge of over 2 e$^-$ mol^{-1} of quinone observed. Compounds **3** and **4** do not show overcharging (i.e., charging is complete at 2 e$^-$ mol^{-1}) or the appearance of lower-potential plateaus during subsequent charging cycles. A loss of capacity on cycling is observed, with the rate of decrease after the first cycle in the order **2 > 1 > 3 >> 4**.

These changes in cell performance on cycling are also apparent from plots of discharge capacity, charge efficiency, and energy efficiency for each cathodic mediator (**Figure 4**). The decline in discharge capacity on cycling for each of the quinones reflects the changes that are apparent in the data presented in Figure 3 and deviate only slightly from what would be predicted based on the NMR solution stability tests. The slower

ADVANCED
SCIENCE NEWS
www.advancedsciencenews.com

ADVANCED
ENERGY
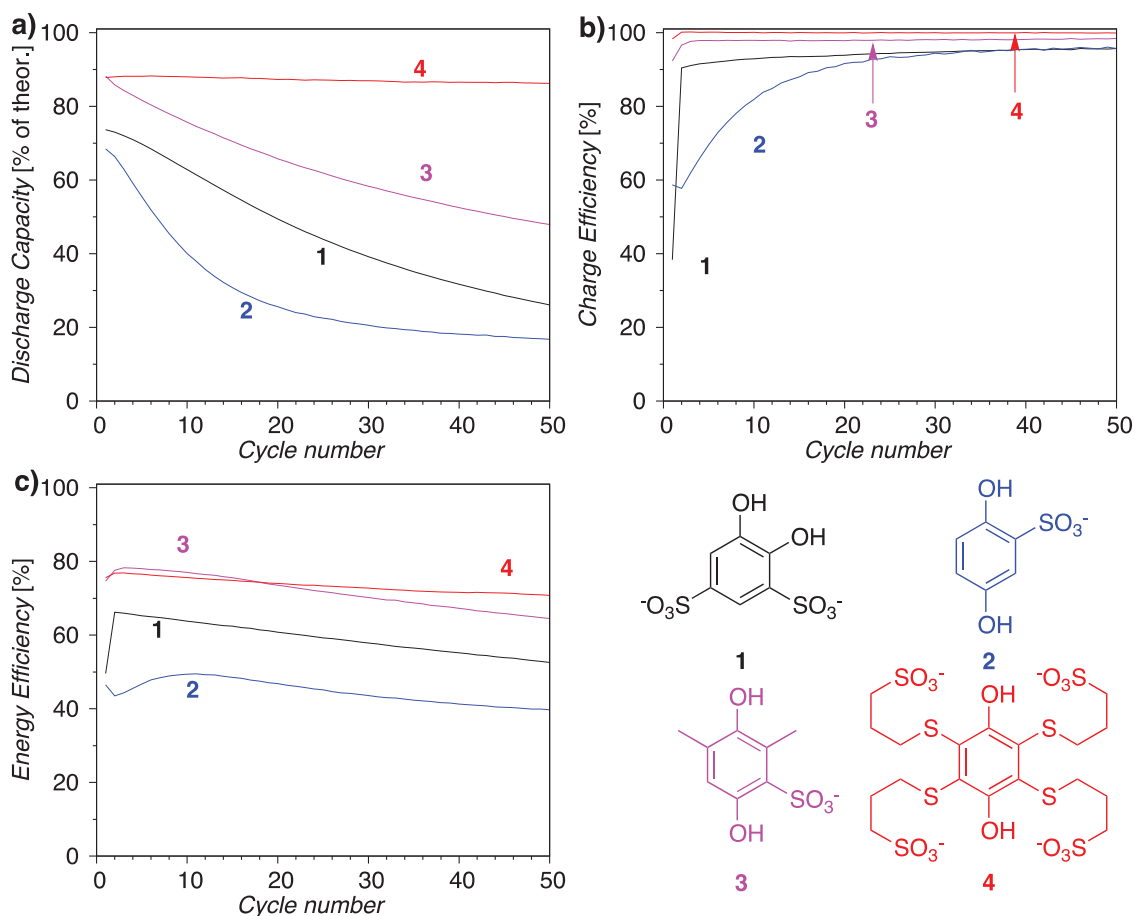MATERIALS
www.advenergymat.de

Figure 4. Plots of discharge capacity (a), charge efficiency (b), and energy efficiency (c) versus cycle number for each of the four cathode mediators.

discharge capacity decline of **1** compared to **2** probably reflects the formation of decomposition products that retain redox-activity, albeit at lower potential (vide infra). The charge efficiency is the ratio of charge passed from discharging relative to charging steps. Values lower than 100% can arise from benign side reactions or irreversible reactions of the charged mediator (i.e., decomposition). In the latter context, even 90% charge efficiency represents a loss of 5% of the available mediator in that cycle if the decomposition process is a two-electron reaction. Energy efficiency reflects not only charge efficiency (irreversible charging is always 0% efficient) but also the ratio between charging and discharging potentials. Thus, **4** displays good energy efficiency despite its low cell potential due to the small difference between charging and discharging potential and the excellent charge efficiency shown in Figure 4b.

Before and after the cycling tests, samples of the anode and cathode solutions were analyzed by NMR spectroscopy (**Table 2**). The decrease in mediator concentration correlated with the results from the quinone stability testing. For compounds **1** and **2**, the decrease in mediator concentration was more extreme than the loss of charge capacity, further indicating that some of the decomposition products retained redox activity. As described above, the anode redox species was maintained in excess and buffered to minimize its effects on the system during the flow battery tests. Since decomposition of quinones by Michael

addition of water will usually produce a hydroquinone that can be oxidized at a lower potential than the starting material (e.g., Scheme S2, Supporting Information), it is essential to have adequate amounts of an anthraquinone present at the anode. Otherwise, the battery will be driven to a state where it cannot be charged since there is no anthraquinone to be reduced, and it cannot be discharged because all of the quinone has undergone Michael addition to form adducts in the hydroquinone oxidation state. The anthraquinone/anthrahydroquinone couple at the anode is further buffered with anthrahydroquinone at the start of the experiment in order to remove the effect of adventitious aerobic oxidation of the anthrahydroquinone.[31]

Following the cycling of compound **4** shown above, the same cell was charged to a nominal 20% state of charge (SOC) and

Table 2. Mediator stability data from RFB tests.

Compound	Loss in RFB discharge capacity [%][a]	Remaining mediator [%][b]
1	48	3.5
2	52	12
3	40	49
4	2[a]/0[c]	98[a]/102[c]

[a]After 50 cycles; [b]Based on ^1H NMR analysis of electrolyte following RFB tests; [c]After 150 cycles total

cycled for a further 100 cycles between 20% and 80% SOC (Figures S18 and S19, Supporting Information), otherwise following the same procedure. Another set of NMR samples was taken following the second period of cycling to further assess the stability of the system. No crossover of any redox-active species was observed following these experiments (Figures S13–S16, Supporting Information).

In addition to the loss of capacity observed during flow battery cycling with some cathode quinones, there was also a shift in the cell potential, especially with compound **1**. We attribute this shift to the formation of mono- and dihydroxyquinones with successively lower reduction potentials. Based on the charge-discharge curves and the extreme instability of oxidized **1** as measured by NMR spectroscopy, it is likely that **1** is converted nearly completely to a monohydroxyquinone during the first cycle, accounting for the drop in charging potential between cycles 1 and 2 and the consumption of $\approx$4 e- mol^{-1} during the initial charge (Figure S13, Supporting Information). This species is then more slowly converted to a dihydroxyquinone, accounting for the gradual appearance of an even lower charging potential.[32] An isomeric dihydroxyquinone was observed to result from oxidation of compound **8**, lending further support to this hypothesis (cf. Scheme S2 and Figure S7, Supporting Information). Similar changes in the identity of the redox-active species during cycling of compound **2** likely contribute to the observed changes to its cell potential. In parallel to these hydroxylation reactions, there are other decomposition reactions that can lead to redox-inactive products and account for the loss of charge capacity with cycling.[21]

The changes in post-experiment concentrations of redox species generally mirror the loss of capacity observed during the experiment (cf. Table 2). The difference between the loss of material and loss of capacity for compounds **1–3** can be explained by the formation of hydroxylation products that retain redox activity, as discussed above.

Compound **4** has a solubility of $\approx$0.25 M in 1 M H$_2$SO$_4$ as the tetrasodium salt. This solubility limits the current density during charging and discharging due to mass-transfer effects. By ion-exchanging **4** to the H$^+$ form, its solubility is improved to over 1 M in water.[33] Simultaneously, the need for an acidic supporting electrolyte on the cathode side is removed.[4] Because **4** dissolves as a tetra-anion and AQDS as a dianion, it was found to be necessary to add H$_2$SO$_4$ to the anode solution in order to approximately balance the ionic strength of the two solutions. The exact additive concentration and identity is a parameter than can be optimized independently of other parameters to produce optimal stability in a fully engineered system.

As a final test, we conducted a RFB experiment using higher concentrations of mediator **4**, accessed via ion-exchange (see Supporting Information). Tests were performed on a larger scale with a 25 cm^2 cell and 1 M solutions of the mediators with 1 M H$_2$SO$_4$ added to the anode solution. The cell was charged to 80% SOC and a power curve was measured with recharging at 50 mA cm^{-2} between data points (**Figure 5**). Repeated measurements showed that the performance was retained (Figure S22, Supporting Information).

The larger-scale tests on the ion-exchanged products demonstrate the performance of a flow battery operating closer to technologically-relevant conditions, albeit still at the cell potential
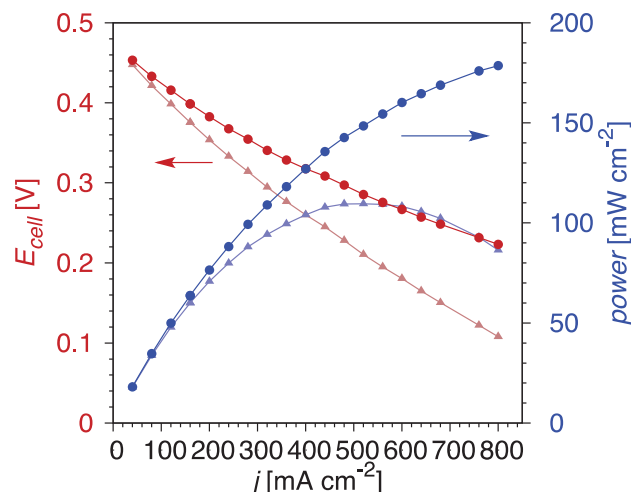

Figure 5. Power curves for aqueous 1 M **4** and 1 M AQDS in 1 M H$_2$SO$_4$ at a 25 cm^2 electrode. Pale curves, triangles are raw data, bright filled circles reflect data with iR-compensation.

imposed by the **4**–AQDS redox couple. At 1 M, the solution viscosity remained low and could be flowed through a 25 cm^2 electrode at rates that supported currents up to 20 A. Under these conditions, a peak power density (iR-corrected) of 180 mW cm^{-2} was obtained and the flow battery retained stable performance on repeated power curve measurements. The observed peak power densities are superior to those reported for other all-quinone redox flow batteries and are within an order of magnitude of the state-of-the-art for inorganic flow batteries.[14,34]

3. Conclusion

Highly soluble, fully-substituted quinones are capable of remarkable stability in aqueous acid. This stability translates into sustained flow battery performance under harsh conditions. The polyanionic nature of **4** inhibits its crossover through proton-exchange membranes while enhancing the solubility of its acid form. Although the reduction potentials of tetrathioether quinones such as **4** and **5** must be increased to become technologically relevant, this study has illustrated the importance of complete substitution of the quinone to achieve stable flow battery performance. That other fully substituted quinones can offer similar stability as well as high potential through careful choice of substituents is easily envisioned and experiments to synthesize such quinones have been initiated.

Supporting Information

Supporting Information is available from the Wiley Online Library or from the author.

Conflict of Interest

The authors have filed patents on some of the compounds and methods described.

Keywords

[1] Z. Yang, J. Zhang, M. C. W. Kinter-Meyer, X. Lu, D. Choi, J. P. Lemmon, J. Liu, *Chem. Rev.* **2011**, *111*, 3577.

[2] G. L. Soloveichik, *Chem. Rev.* **2015**, *115*, 11533.

[3] J. D. Hofmann, D. Schröder, *Chem. Ing. Tech.* **2019**, *91*, 786.

[4] J. D. Milshtein, R. M. Darling, J. Drake, M. L. Perry, F. R. Brushett, *J. Electrochem. Soc.* **2017**, *164*, A3883.

[5] J. Noack, N. Roznyatovskaya, T. Herr, P. Fischer, *Angew. Chem., Int. Ed.* **2015**, *54*, 9776.

[6] M. Imtiaz, M. S. Rizwan, S. Xiong, H. Li, M. Ashraf, S. M. Shahzad, M. Shahzad, M. Rizwan, S. Tu, *Environ. Int.* **2015**, *80*, 79.

[7] a) X. Wei, W. Pan, W. Duan, A. Hollas, Z. Yang, B. Li, Z. Nie, J. Liu, D. Reed, W. Wang, V. Sprenkle, *ACS Energy Lett.* **2017**, *2*, 2187; b) P. Leung, A. A. Shah, L. Sanz, C. Flox, J. R. Morante, Q. Xu, M. R. Mohamed, C. Ponce de León, F. C. Walsh, *J. Power Sources* **2017**, *360*, 243; c) J. Luo, B. Hu, M. Hu, Y. Zhao, T. L. Liu, *ACS Energy Lett.* **2019**, *4*, 2220.

[8] M. T. Huynh, C. W. Anson, A. C. Cavell, S. S. Stahl, S. Hammes-Schiffer, *J. Am. Chem. Soc.* **2016**, *138*, 15903.

[9] a) S. Er, C. Suh, M. P. Marshak, A. Aspuru-Guzik, *Chem. Sci.* **2015**, *6*, 885; b) S. D. Pineda Flores, G. C. Martin-Noble, R. L. Phillips, J. Schrier, *J. Phys. Chem. C* **2015**, *119*, 21800.

[10] Y. Ding, C. Zhang, L. Zhang, Y. Zhou, G. Yu, *Chem. Soc. Rev.* **2018**, *47*, 69.

[11] Phenazines are another emerging class of $2H^+/2e^-$ mediators, see for instance: A. Hollas, X. Wei, V. Murugesan, Z. Nie, B. Li, D. Reed, J. Liu, V. Sprenkle, W. Wang, *Nat. Energy* **2018**, *3*, 508.

[12] It is also possible to use a single molecule containing both redox-active moieties. For a quinone-based example, see: L. Tong, Y. Jing, R. G. Gordon, M. J. Aziz, *ACS Appl. Energy Mater.* **2019**, *2*, 4016.

[13] B. Huskinson, M. P. Marshak, C. Suh, S. Er, M. R. Gerhardt, C. J. Galvin, X. Chen, A. Aspuru-Guzik, R. G. Gordon, M. J. Aziz, *Nature* **2014**, *505*, 195.

[14] L. Hoober-Burkhardt, S. Krishnamoorthy, B. Yang, A. Murali, A. Nirmalchandar, G. K. Surya Prakash, S. R. Narayanan, *J. Electrochem. Soc.* **2017**, *164*, A600.

[15] B. Yang, L. Hoober-Burkhardt, S. Krishnamoorthy, A. Murali, G. K. Surya Prakash, S. R. Narayanan, *J. Electrochem. Soc.* **2016**, *163*, A1442.

[16] B. Yang, L. Hoober-Burkhardt, F. Wang, G. K. Surya Prakash, S. R. Narayanan, *J. Electrochem. Soc.* **2014**, *161*, A1371.

[17] S. Zhang, X. Li, D. Chu, *Electrochim. Acta* **2016**, *190*, 737.

[18] A. Murali, A. Nirmalchandar, S. Krishnamoorthy, L. Hoober-Burkhardt, B. Yang, G. Soloveichik, G. K. Surya Prakash, S. R. Narayanan, *J. Electrochem. Soc.* **2018**, *165*, A1193.

[19] B. Hu, J. Luo, M. Hu, B. Yuan, T. L. Liu, *Angew. Chem., Int. Ed.* **2019**, *58*, 16629.

[20] B. Huskinson, S. Nawar, M. R. Gerhardt, M. Aziz, *ECS Trans.* **2013**, *53*, 101.

[21] a) H. Erdtman, H.-E. Högberg, *Tetrahedron* **1979**, *35*, 535; b) H. Erdtman, *Proc. R. Soc. Ser. A* **1933**, *143*, 177; c) H. Erdtman, *Proc. R. Soc. Ser. A* **1933**, *143*, 191; d) H. Erdtman, *Proc. R. Soc. Ser. A* **1933**, *143*, 223; e) H. Erdtman, *Proc. R. Soc. Ser. A* **1933**, *143*, 228.

[22] We have recently described compound **4** and its utility in a mediated fuel cell cathode: Y. Preger, J. B. Gerken, S. Biswas, C. W. Anson, M. R. Johnson, T. W. Root, S. S. Stahl, *Joule* **2018**, *2*, 2722.

[23] For an efficient synthesis of **4** and **5**, see: J. B. Gerken, A. G. Stamoulis, S.-E. Suh, N. D. Fischer, Y.-J. Kim, I. A. Guzei, S. S. Stahl, *Chem. Commun.* **2020**, *56*, 1199.

[24] T. H. James, A. Weissberger, *J. Am. Chem. Soc.* **1939**, *61*, 442.

[25] MWCNT-coating of the glassy carbon electrode was found to be necessary to enhance electron-transfer kinetics. For more detail, see the supporting information to ref. [22].

[26] E. Bosch, R. Rathore, J. K. Kochi, *J. Org. Chem.* **1994**, *59*, 2529.

[27] Initial flow battery experiments were conducted with alizarin red sulfonate at the anode to improve the cell potential; however, alizarin red sulfonate has limited solubility (cf. ref. [29d]). In these experiments, the apparatus became clogged by an insoluble decomposition product after a few cycles. Presumably, the results obtained in ref. [17] were possible through operating at room temperature and for only three charge–discharge cycles. A recent computational paper suggests some possible decomposition pathways of this compound: D. P. Tabor, R. Gómez-Bombarelli, L. Tong, R. G. Gordon, M. J. Aziz, A. Aspuru-Guzik, *J. Mater. Chem. A* **2019**, *7*, 12883.

[28] The best price of sodium 2-mercaptoethanesulfonate ($95.10 / 10.g) is a factor of 11.4 higher (10.5× on mole, rather than mass, basis) than sodium 3-mercaptopropanesulfonate ($83.10 / 100. as offered by the same supplier: https://www.sigmaaldrich.com/catalog/product/mm/810595?lang=en&region=US and https://www.sigmaaldrich.com/catalog/product/aldrich/251682?lang=en&region=US (accessed: January 2020).

[29] a) M. Phillips, *Chem. Rev.*. **1929**, *6*, 157; b) A. M. Dawson, A. Johnson, *J. Soc. Dyers Colour.* **1966**, *82*, 49; c) A. Socha, *Dyes Pigm.* **1990**, *12*, 213; d) K. Wedege, E. Dražević, D. Konya, A. Bentien, *Sci. Rep.* **2016**, *6*, 39101.

[30] A similar charge-hold-discharge cycle has recently been reported as a means of stability-testing flow battery mediators: M.-A. Goulet, M. J. Aziz, *J. Electrochem. Soc.* **2018**, *165*, A1466.

[31] Although we believe that aerobic oxidation did not occur in the tests described here, initial experiments where silicone tubing was used created an inadvertent membrane reactor and served to illustrate the importance of eliminating the effect of adventitious oxidation on cathode stability comparisons. There are also reports of instability of sulfonated anthra(hydro)quinones in acidic aqueous solution, see ref. [29].

[32] Compare with refs. [14, 15, 22] (specifically Scheme S8 and associated text in the supporting information to this reference), and ref. [29d].

[33] Accurate solubility testing is complicated by the tendency of the acidic form of compound **4** to supersaturate, but cell cycling tests show that it must be at least 1 M based on the absence of any precipitate in the fully-charged state.

[34] a) M. L. Perry, R. M. Darling, R. Zaffou, *ECS Trans.* **2013**, *53*, 7; b) T. J. Davies, J. J. Tummino, *C* **2018**, *4*, 8.